

# Machine Learning Algorithms for Retinal Image Analysis and Glaucoma Detection

Syed Akhter Hussain  
Computer Science and Engineering  
Department  
Hi-Tech Institute of Technology  
Aurangabad Maharashtra India  
akhter.it@gmail.com

Pratap Mohanrao Mohite  
Computer Science and Engineering  
Department  
Hi-Tech Institute of Technology  
Aurangabad Maharashtra India  
Pratapmohite1989@gmail.com

Sandip Eknathrao Ingle  
Computer Science and Engineering  
Department  
Hi-Tech Institute of Technology  
Aurangabad Maharashtra India  
seingle@gmail.com

Mohammad Waseem Ahmed Siddiqui  
Computer Science and Engineering Department  
Hi-Tech Institute of Technology  
Aurangabad Maharashtra India  
wassid09@gmail.com

Mohammed Zeeshan Raziuddin  
Computer Science and Engineering Department  
CSMSS College of Engineering  
Aurangabad Maharashtra India  
zeeshan.shaikh@gmail.com

**Abstract**—In recent years machine learning technology are widely used in modern biomedical imaging systems to recognise and classify a wide range of human disorders. The development of a retinal image analysis system requires precise segmentation. In this work we are using fully connected conditional random field model to overcome energy minimization problem as compare to pots model which is limited for elongated retinal structure as it takes pairwise potential which in turn low priority for vessel segmentation. In this work parameters learned automatically by structured output support vector machine and gives structured predictions we use publically available data sets DRIVE, STARE, HRF and CHASEDB1 to train our system, after segmentation we are classify them with the help of support vector machine and K-nearest neighbour machine learning algorithms to get accurate results. We compare and validate our result with respect to sensitivity, specificity, precision, time complexity and F1 score performance metrics.

**Index Terms**—Retinal image, SVM, K-NN, segmentation, FC-CRF.

## I. INTRODUCTION

Glaucoma is leading eye disease in today's world that leads to vision lost. Glaucoma occurs due to increase in intraocular pressure of human eye which damages optic nerve head. It manages visual information to the brain. When intraocular pressure rises due to hypertension or a malfunction of the eye drainage system, aqueous humor flows between the cornea and lens, and vitreous humor is present in a rare part of the eye ball. Aqueous humor nourishes and removes the wastage and responsible to maintain intraocular pressure, vitreous humor holds the eyeball and maintains its shape and size. If pressure continues it damages optic nerve head, glaucoma will cause everlasting vision lost. Clinical screening had certain flaws, and according to the WHO, 285 million individuals were visually endangered, with 39 million being blind and 246 million having poor vision [1]. In India, there are approximately 11.2 million people suffering from glaucoma and other eye diseases. 6.48 million people are expected to have primary open angle glaucoma, and 2.54 million people have primary angle-closure glaucoma. Around 65% of people with low vision and 82% of people who are

older than 50 years are blind [2]. 26 million people in Latin America had limited eyesight, and 3.2 million were blind [3]. Similar types of data are seen throughout Europe [4]. Researchers estimated in their study [5, 6] that the rest of the globe suffers from glaucoma, diabetic retinopathy, and age-related macular degeneration. Fundus photo graphs are a type of medical imaging technique that is used to identify eye diseases. They are non-invasive and simple to execute since they are computer-aided [7]. Manual analysis is a time-consuming method since ophthalmologists must perform and verify multiple fundus photographs with varying degrees of parameters, and diagnosis may change from one expert to the next based on their expertise and skills [8]. The objective of retinal image analysis is to generate qualitative data for clinical evaluation. Ophthalmologists require both qualitative and quantitative retinal vascular impressions.

## II. LITERATURE REVIEW

Over the last decade, there has been a lot of focus on the topic of automated segmentation of retinal blood vessels [9]. All previous work on vascular segmentation is based on supervised and unsupervised approaches. Unsupervised approaches are dominated by matched filtering, vessel tracking, morphological changes, and model-based algorithms. A 2-D linear structuring element is used to generate a Gaussian intensity profile of the retinal blood vessels. Employing Gaussians and their derivatives for vessel enhancement [10]. The structuring element is rotated 8-12 times to suit the vessels in various configurations in order to extract the border of the vessel. Because a halting condition is examined for each end pixel, this approach has a significant temporal complexity. Another vessel tracking approach is [11]. Gabor filters are used for detecting and extracting blood vessels. Because of the insertion of a significant number of erroneous edges, this approach suffers from over detection of blood vessel pixels [12]. A morphology-based technique for center-line identification combines morphological modifications with curvature information and matched-filtering. Be-

cause of the center-line detection of the vessel and the subsequent vessel filling operation, this approach has a high temporal complexity and is vulnerable to false edges caused by bright area edges such as optic discs and exudates describes perceptual transformation algorithms for segmenting veins in retinal pictures with bright and red lesions [13]. Active contour models are used in another model-based vascular segmentation method suggested in [14], although it again has computational complexity issues. Additionally, neighborhood analysis and gradient-based data are used by multi-scale vessel segmentation algorithms presented in [15-16] to identify the vessel pixels. All of these unsupervised techniques are either computationally demanding or sensitive to abnormalities in the retina. Pixels are divided into vessel and nonvessel groups using the supervised vessel segmentation methods. Authors in [17] presented, a 31-feature set collected using the derivatives of Gaussians for  $k$ -nearest neighbor ( $k$ -NN) classifier. The method described in [18] was enhanced by the use of ridge-based vessel detection. Here, the picture is divided by naming the nearest ridge member for each pixel. A 27 feature set is then calculated for each pixel and utilised by a  $k$ -NN classifier. The vastness of the feature sets slows down both of these procedures. Additionally, these techniques depend on training data and are vulnerable to spurious edges. Another approach described in [19] makes use of a Gabor-wavelet-extracted six-feature set and a Gaussian mixture model (GMM) classifier. This approach also depends on training data, and it takes hours to train GMM models using a mixture of 20 Gaussians. Line operators and a support vector machine (SVM) classifier with a three-feature set per pixel are used in the technique described in [20]. Due to the SVM classifiers, this approach is computationally demanding and particularly sensitive to the training data. In several applications, conditional random fields (CRFs) are widely utilised for picture segmentation [21,22,23]. To our knowledge, they have never been used to segment blood vessels in fundus images.. This is probably because the elongated structures that make up a vascular segmentation are given a low prior by the common pairwise potentials, like those in a Potts model. Due to this feature, we developed a unique blood vessel segmentation approach based on completely linked CRFs [24].

### III. METHOD

Early glaucoma detection and classification will enable patients to receive appropriate care and assistance from their eye surgeons, thereby improving their standard of living.

#### A. Vascular Segmentation by CRF

Conditional Random Fields approach is a statistical modelling technique in which pixel mapping is done in graph form. In the CRFs model, each pixel is considered as a node and is connected to other nodes that form the edge according to connectivity rules [25, 26, 27], so the segmentation task in this technique is posed as an energy minimization problem. Local neighborhood based CRFs vary from Fully Connected CRFs in that earlier, 4 pixel neighborhood connectivity is followed by each node [28], but in the latter, every node is understood to be related to every other pixel in the fundus picture.

Here  $y = \{y_i\}$  a labeled pixels of the image  $I$  in label space  $L = \{-1, 1\}$ , where 1 is considered as retinal blood vessels and -1 extra class. Characterization of conditional random field  $(I, y)$  is done by Gibbs distribution:

$$p(Y|I) = \frac{1}{Z(I)} \exp\left(-\sum_{c \in C_G} \phi_c(Y_c|I)\right) \quad (1)$$

$Z(I)$  is the normalization constant,  $G$  is the image graph associated with  $I$ , and  $CG$  is the set of cliques., with potential  $\phi_c$  [23]. Gibbs energy function can be derived from following Equation:

$$E(Y|I) = \sum_{C \in C_G} \phi_C(Y_C|I) \quad (2)$$

Energy minimization is performed for labeling that is the maximum a posteriori simply it is called MAP:

$$y^* = \underset{Y \in L}{\text{arg min}} E(Y|I) \quad (3)$$

Binary segmentation of the vasculature derives from the minimization of  $E(Y|I)$ . To denote  $\phi_c(Y_c|I)$ , we use  $\psi_c(y_c)$ . Additionally, unary and pairwise potentials energy decompositions are regarded as higher order potentials [29]. Total energy is obtained by adding the unary potential and pairwise potential.

$$E(Y) = \sum_i \psi_u(y_i, x_i) + \sum_{(i,j) \in C_G} \psi_p(y_i, y_j, f_i, f_j) \quad (4)$$

$k^{(m)}$  is defined as rigid function based on arbitrary feature, linear combination of weight is defined as  $f^{(m)}$ ,  $w_p^{(m)}$  and  $\mu(y_i, y_j)$  defined the label compatible function.  $f^{(m)}$  is traced similarity in between connected pixels determine by Gaussian kernels. It is obtained by connectivity rule applied on pixels neighbors by using conditional random field formulation. Compatible function is defined by  $\mu$ , Parameters  $w_u$ ,  $w_p^{(m)}$  employed to manage the unary features' weight as well as pairwise kernels with respect to energy function in addition, and learning of bias is defined by  $w_\beta$ .

Furthermore Gridiron diagrams above define LNB-CRFs. Accordingly, each pixel is considered to be connected to its four related neighbors through an edge in this technique. According to paired potentials provided as an  $m^{\text{th}}$  pairwise feature, the function is derived as follows:

$$K^{(m)}(f_i^{(m)}, f_j^{(m)}) = \frac{|f_i^{(m)} - f_j^{(m)}|}{2_{(m)}^\theta} \quad (5)$$

where  $(m)$  is a bandwidth that controls the weight of pixel feature differences. By using the mincut/max-flow strategy, the grid approach's energy consumption is minimised.

Finally the FC-CRF model is represented in graphical form, where each pixel in the image is connected to other pixels this is the highest ordered potential it is also used to trace long-range interactions between image pixels. It is advantageous in the segmentation process because it helps to improve accuracy, but it has limitations with inference. Recently authors in [30] presented a competent inference approach by taking pairwise potential and mean field approximation of CRF, which helped to perform accurate segmentations in a matter of seconds. The FC-CRF's pairwise kernels are as follows:

$$k^{(m)}(f_i^{(m)}, f_j^{(m)}) = \exp\left(\frac{-|p_i - p_j|^2}{2\theta_p^2} - \frac{|f_i^{(m)} - f_j^{(m)}|^2}{2\theta_m^2}\right) \quad (6)$$

In this equation  $p_i$  and  $p_j$  are defined as co-ordinate vectors of pixels respectively. Kernel widths control the degree weight defined as  $\theta_p$  and  $\theta(m)$ . For instance, when increase in lengthy interactions observed by  $\theta_p$  and vice versa for local neighborhoods. In the same way, when  $\theta(m)$  increases tolerance is higher with respect to  $m$ th feature and vice versa for lowering the tolerance successively.

### B. Learning of CRFs by SOSVM

In order to learn  $w = (w_u, w_\beta, w_p)$ , where  $w_u, w_\beta$  and  $w_p$  are the weights of unary potential over bias term and pairwise kernel the approach is not suitable for high dimensional features. To overcome this we are employing SVM, a supervised learning approach that enforces the 1-slack formulation in terms of margin rescaling, as recommended in [31].  $S = \{(s^{(1)}, y^{(1)}), \dots, (s^{(n)}, y^{(n)})\}$  is the training set. Here,  $y^{(i)}$  is  $i$ th image,  $x^{(i)}$  is unary potential feature set,  $f^{(i)}$  is pairwise potential feature set,  $s^{(i)}$  is training set containing both unary and pairwise features. Hence to get weights  $W$  we have to use following formulation:

$$\min_{w, \xi \geq 0} \frac{1}{2} \|w\|^2 + C\xi \quad (7)$$

Put through

$$\forall (y^{-(1)}, y^{-(n)}): \sum_{i=1}^n \langle w, \psi(s^{(i)}, y^{(i)}) - \psi(s^{(i)}, y^{-(i)}) \rangle \geq \sum_{i=1}^n \Delta(y^{(i)}, y^{-(i)} - \xi) \quad (8)$$

$C$  is defined as regularization constant;  $\xi$  is a slack variable with respect to constraints  $y^{(i)}$ , for labeled  $y$  feature map is defined as  $\phi(s, y)$ ; and to measures loss of function we defined  $\Delta(y, y^-)$ ,  $\Delta$  is nothing but Hamming loss formulate as follows:

$$\Delta(y, y^-) = \sum_i [y_i \neq y_i^-] \quad (9)$$

Contained in the brackets is Prediction of labeling with respect to segmentations gold standard, feature map is formulated as follows:

$$\varphi(s, y) = (\sum_k \varphi_u(x_k, y_k), \sum_k \varphi_\beta(\beta, y_k), \sum_k \sum_{j < k} \varphi_p(y_k, y_j, f_k, f_j)) \quad (10)$$

$\varphi_u$  unary feature map sum,  $\varphi_\beta$  bias feature map,  $\varphi_p$  pairwise feature map.

Binary vector  $\varphi(y_i) \in \{0, 1\}^{|I|}$  as:

$$\varphi_y(y_i) = \begin{cases} (1, 0) & \text{if } y_i = -1 \\ (0, 1) & \text{if } y_i = 1 \end{cases} \quad (11)$$

Feature maps obtained individually defined as follows:

$$\varphi_u(x_k, y_k) = x_k \otimes \varphi_y(y_k) \quad (12)$$

$$\varphi_\beta(\beta, y_i) = \beta \varphi_y(y_i) \quad (13)$$

$$\forall m: [\varphi_p(y_k, y_j, f_k, f_j)]_m = \mu(y_i, y_j) k^{(m)}(f_i^{(m)}, f_j^{(m)}) \quad (14)$$

$\otimes$  Is kronecker product, hence using cutting plane technique is applied on equation (7) as author presented this efficient technique [30-31].

### C. Features for Segmentation and Classification

We employed a different strategy for feature extraction for blood vessel segmentation in retinal vessels [32]. Demonstrated multiscale line detectors with regard to 2D Gabor wavelets applied to unary potentials, as in [33] vessels are amplified in fundus pictures for paired potentials as indicated in [34]. Similarly, authors in [35] discuss many features. Authors in [36,37] provide a systematic explanation of the feature extraction procedure, which is based on a grey level scale. Furthermore, authors recommended range of view for selected characteristics to minimise erroneous detection. As a result, the FOV mask is in charge of removing erroneous detection

### D. Scaling Retinal Images to Various Resolution

We adjust the weights of unary features as well as pairwise kernels for effective characterization of retinal vasculature, as we know that retinal structure has low dense potentials, so obtained features are more sensitive during calibration with respect to retinal image pixel. The 2D Gabor wavelet is used for scaling. Similarly, Authors in [32] present a Line detection algorithm, and authors in [34] presents enhancing strategy is proportional to the linear structured component because poor resolution these parameters are set for DRIVE dataset [18]. Because the method is not proportionately scaled, performance will suffer if these settings are used to high quality Images The benefit of these characteristics is the shift in orientation caused by Change in angle has no effect on the pixel resolution of the retinal fundus picture the same performance may be predicted for preprocessing of feature parameters such as the measurement of the median filter for background estimation, or range of the opening pretend by boundary development. For this parameter  $\theta_p$ , which is used in pairwise potential connections with qualifying distance of each image pixel, FC-CRF is impacted by pixel image resolution considered with pairwise potential.

### E. Machine Learning Algorithms for Classification

In this presented work we used SVM and K-NN classification algorithms for glaucoma detection.

#### 1) SVM

In our work, we can define support vector machines as support vector classifiers. Kernels (similarity quantifiers) are used to broaden the feature space in this case. The classification and regression analysis are done using the supervised learning approach and the analysed data. In our scenario, non-linear classification is required to deal with large dimensions. We tweak the following settings for this goal.

- Kernel parameter:-determines whether the separation is linear or non-linear.
- Regularization parameter:- This parameter is in responsible for SVM optimisation during the training phase, calculating the number of misclassifying avoided spots.

- Gamma parameter:-defines the influence in the training phase that is low (far) or high (near).
- Line separation for high class points using the margin parameter.

#### 2) *k*-NN

It is a supervised classification strategy that trains the closest feature space and separates datasets into two sets. Each row has *k* closest training sets of pixels resolution, and categorization is done using a majority of votes. *K*-NN works by calculating distances between training and testing data vectors using the Euclidian distance formulation the number *K* denotes related identified neighbors. When *k*=1, we name it the nearest neighbor algorithm since we acquire the closest training samples.

### IV. MATERIALS AND ASSESMENT

Evolution and validation of our work is explained in this section.

#### A. Datasets

We have used different types of data set for training purpose mentioned following.

TABLE I. DATASETS

Dataset	Capturing Angle	Resolution
DRIVE[18]	45° FOV	565 × 584 with 8 bits per color channel
CHASEDB1 [38]	35° FOV	700 × 605 pixels with 8 bits per color channel
STARE [10]	30° FOV	1280 × 960 pixels with 8 bits per color channel
HRF [39, 40]	60° FOV	resolution 3304 × 2336 pixels

#### B. Gold Standard Metric for Evolution

We compared our segmentation results to the gold standard labeling available for datasets. Quality of findings based on seven specific dimensions in terms of true positive, true negative, false positive, and false negative, which are described as TP, TN, FP, and FN concurrently and taking into account pixels existing inside field of view.

$$S_e = \frac{TP}{TP + FN} \quad (15)$$

$$S_p = \frac{TN}{TN + FP} \quad (16)$$

$$P_r = \frac{TP}{TP + FP} \quad (17)$$

$$Tx = (x-1) \quad (18)$$

$$F_1 = \frac{2 \cdot P_r \cdot R_e}{P_r + R_e} \quad (19)$$

### V. RESULTS

In this section, we present a detailed study of our automated segmentation system for the detection of various eye-

related diseases, as shown in Figure 1. We perform segmentation on the DRIVE dataset, and moving forward, we apply it to the CHASEDB1 dataset, as depicted in Figure 2. The segmentation results for the STARE dataset are presented in Figure 3, and for the HRF dataset, segmentation results are shown in Figure 4. In the initial stage, we conducted a comprehensive study of different eye diseases, understanding their occurrence and their impact on human eyes. Afterward, we calibrated them using image processing techniques, collecting all the necessary parameters for our work, which are summarized in TABLE II and TABLE III here we observe that *K*-NN Classification algorithm works more effectively than SVM Classification algorithm as shown in Figure 5 and Figure 6 respectively. For retinal vessel segmentation, we employed a fully connected conditional random field model, specifically chosen due to the dense and elongated structure of retinal vessels, where unary and pairwise potentials are crucial. We then classified the segmented vessels using supervised learning techniques, employing both Support Vector Machine (SVM) and *K*-Nearest Neighbors (*K*-NN) classification algorithms.

#### A. Segmentation results on DRIVE data set.

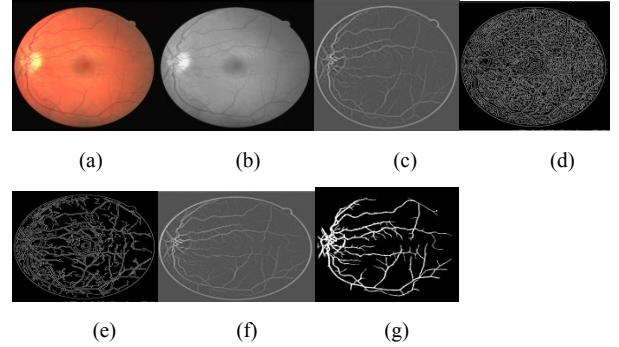


Figure 1. Segmentation Results on DRIVE (a) Input image (b) gray scale image (c) Eigen enhanced image (d) Wavelet enhanced image output (e) local enhanced image output (f) Background normalization (g) Vessel segmentation result.

#### B. Segmentation results on CHASEDB1 dataset

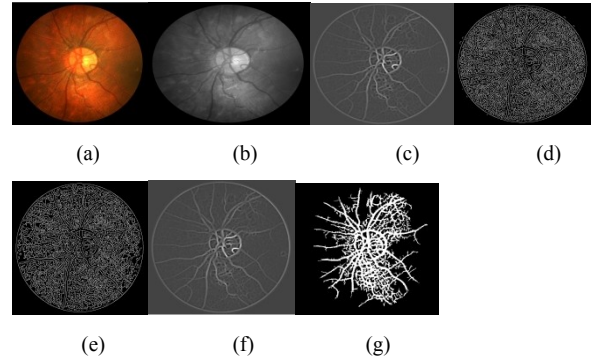


Figure 2. Segmentation Results on CHASEDB1 (a) Input image (b) gray scale image (c) Eigen enhanced image (d) Wavelet enhanced image output (e) local enhanced image output (f) Background normalization (g) Vessel segmentation result.

C. Segmentation results on STARE dataset

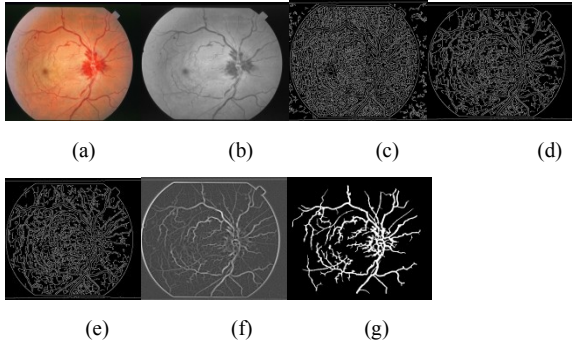


Figure 3. Segmentation Results on STARE (a) Input image (b) gray scale image (c) Eigen enhanced image (d) Wavelet enhanced image output (e) local enhanced image output (f) Background normalization (g) Vessel segmentation result.

D. Segmentation results on HRF dataset

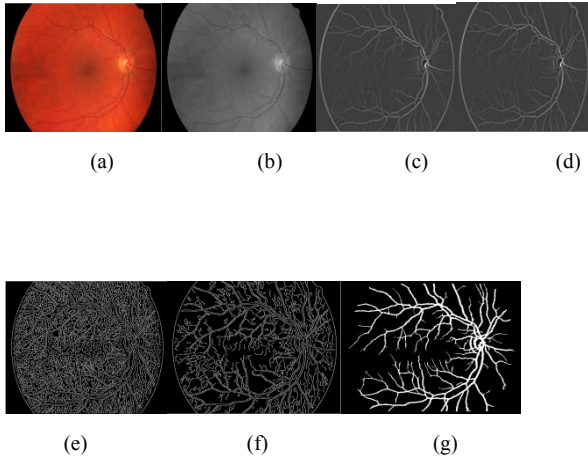


Figure 4. Segmentation Results on HRF (a) Input image (b) gray scale image (c) Eigen enhanced image (d) Wavelet enhanced image output (e) local enhanced image output (f) Background normalization (g) Vessel segmentation result.

TABLE II. AVERAGE PERFORMANCE ANALYSIS OF K-NN ALGORITHM

Data Set	$S_e$	$S_p$	$P_r$	F1	$T_x$ (sec)
DRIVE	.9334	.9049	.8512	.8903	55
CHASEDB1	.9334	.9063	.8518	.8907	52
STARE	.9334	.9063	.8560	.8929	54
HRF	.9334	.9045	.8544	.8921	52

TABLE III. AVERAGE PERFORMANCE ANALYSIS OF SVM ALGORITHM

Data Set	$S_e$	$S_p$	$P_r$	F1	$T_x$ (sec)
DRIVE	.4600	.7818	.8000	.5841	203
CHASEDB1	.4534	.9063	.7809	.5737	194
STARE	.4667	.7818	.8000	.5894	75
HRF	.4800	.7818	.8000	.6000	75

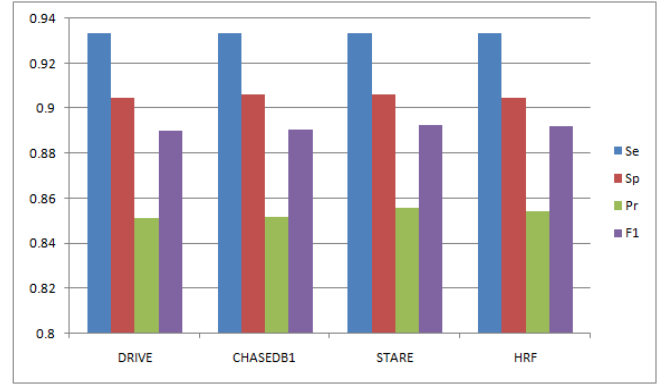


Figure 5. Performance graph of K-NN Algorithm

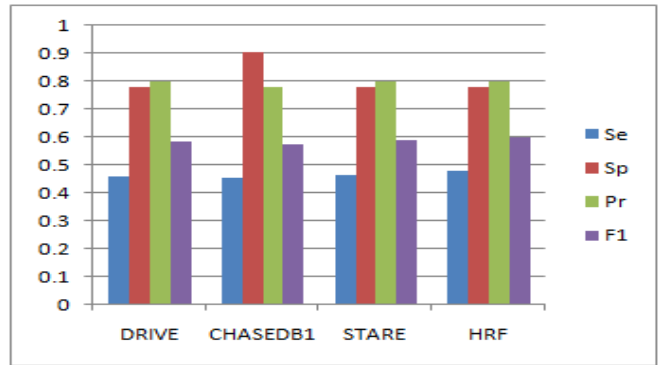


Figure 6. Performance graph of SVM Algorithm

VI. CONCLUSION

This paper presents the retinal Image analysis and comprehensive machine learning algorithm for segmentation and detection of glaucoma using fully connected random filed model, feature extraction and retinal vasculature reconstruction is more effectively obtained than using unary potential or a local neighborhood based conditional random filed. The efficiency is assessed in terms of sensitivity, specificity, and precision. In this presented work K-NN algorithm is worked superior then SVM algorithm. Our retinal vessel segmentation results on DRIVE, STARE, CHASEDB1 and HRF shows expressive performance on dense potentials. Further they can be used for numerous biomedical and biological applications for identification and detection of various problems.

ACKNOWLEDGMENT

I would like to express my heartfelt appreciation to my research supervisor, Dr. Ratnadeep R Deshmukh, Professor, Department of Computer Science and IT. Dr. Babasaheb Ambedkar of Marathwada University, Aurangabad, for his ongoing support for research.

REFERENCES

[1] Sixty-Sixth World Health Assembly “Towards universal eye health: a global action plan 2014–2019” of WHO <https://www.emro.who.int/>.

- [2] R.George,Ramesh S,ve,Lingam Vijaya “Glaucoma in India:estimetaed burden of disease” in Journal of Glaucoma august 2010 volume 19 issue 6 p 391-397.
- [3] C.F.Etienne “Reducing avoidable blindness and visual impairment in the region of the America”in Pan American Journal of Public Health,37(1):1-3,2015.
- [4] E.Prokofyeva and Eberhartz zerenner “Epidemology of major eye diseases leading to blindness in Europe: A literature review” in Ophthalmic Research,47(4):171-188,2012.
- [5] Jannet Leasher,Rupert Bourne,Seth R flaxman and Jos B Jonas”Global estimates on the number of people blind or visually impaired by diabetic retinopathy: A meta-analysis from 1990-2010” in Diabetes care 39(9):1643-1649.
- [6] Y.C.Than et al. “Global prevalence of glaucoma and projection of glaucoma burden through 2040: a systematic review and meta-analysis” in Ophthalmology, 121 (11):2081-2090, 2014.
- [7] M.D.Abramoff,Mona K Garvin and Milan Sonka”Retinal imaging and image analysis” in IEEE Reviews Biomedical Engineering, 3:169-208, 2010.
- [8] M.D.Abramoff and Nemijer”Mass screening of Diabetic retinopathy using automated methods” in Springer pp 41-50 September, 2015.
- [9] M. Fraz et al.“Blood vessel segmentation methodologies in retinal images a survey,” in Computer. Methods and Programs Biomedicine., vol. 108, no. 1, pp. 407–433, 2012.
- [10] A. Hoover, V. Kouznetsova, and M. Goldbaum, “Locating blood vessels in retinal images by piecewise threshold probing of a matched filter response,” *IEEE Trans. Med. Imag.*, vol. 19, no. 3, pp. 203–210, Mar. 2000.
- [11] R. Rangayyan, F. Oloumi, F. Oloumi, P. Eshghzadeh-Zanjani, and F. Ayres, “Detection of blood vessels in the retina using gabor filters,” in *Proc. Canadian Conf. Electr. Comput. Eng.*, 2007, pp. 717–720.
- [12] A. Mendonca, and A. Campilho, “Segmentation of retinal blood vessels by combining the detection of centerlines and morphological reconstruction,” in *IEEE Trans. Med. Imag.*, vol. 25, no. 9, pp. 1200–1213, Sep. 2006.
- [13] Benson S.Y. Lam, Yongasheng Gao and Alan Wee-Chung Liew “General retinal vessel segmentation using regularization-based multiconcavity modeling,” *IEEE Trans. Med. Imag.*, vol. 29, no. 7, pp. 1369–1381, Jul. 2010.
- [14] B. Al-Diri, A. Hunter, and D. Steel, “An active contour model for segmenting and measuring retinal vessels,” in *IEEE Trans. Med. Imag.*, vol. 28, no. 9, pp. 1488–1497, Sep. 2009.
- [15] A. Budai, G. Michelson, and J. Hornegger, “Multiscale blood vessel segmentation in retinal fundus images,” in *Proc. Bildverarbeitung fr die Med.*, pp. 261–265, Mar. 2010
- [16] A. Budai, R. Bock, A. Maier, J. Hornegger, and G. Michelson, “Robust vessel segmentation in fundus images,” in *Int. J. Biomed. Imag.*, article 154860, 2013.
- [17] M. Niemeijer, J. Staal, B. van Ginneken, M. Loog, and M. D. Abramoff, “Comparative study of retinal vessel segmentation methods on a new publicly available database,” in *Proc. SPIE*,vol. 5370, pp. 648–656, 2004.
- [18] J. Staal, M. Abramoff, M. Niemeijer, M. Viergever, and B. van Ginneken, “Ridge-based vessel segmentation in color images of the retina,” in *IEEE Trans. Med. Imag.*, vol. 23, no. 4, pp. 501–509, Apr. 2004.
- [19] J. Soares, J. Leandro, R. Cesar, H. Jelinek, and M. Cree, “Retinal vessel segmentation using the 2-D Gabor wavelet and supervised classification” in *IEEE Trans. Med. Imag.*, vol. 25, no. 9, pp. 1214–1222, 2006.
- [20] E. Ricci, and R. Perfetti, “Retinal blood vessel segmentation using line operators and support vector classification,” in *IEEE Trans. Med. Image.*, vol. 26, no. 10, pp. 1357–1365, Oct. 2007.
- [21] Xuming He, Richard Zemel and M.A Carriera perpinan “Multiscale conditional random fields for image labeling,” in *Computer Vision and Pattern Recognition, 2004. CVPR 2004. Proceedings of the 2004 IEEE Computer Society Conference on*, vol. 2. IEEE, 2004, pp. II–695.
- [22] S. Kumar and M. Hebert, “Discriminative random fields,” in *Int. J. Comput. Vision*, vol. 68, no. 2, pp. 179–201, Jun. 2006.
- [23] S. Z. Li, “Markov Random Field Modeling in Image Analysis” in 3rd ed. Springer, 2009.
- [24] J. I. Orlando and M. Blaschko, “Learning fully-connected CRFs for blood vessel segmentation in retinal images,” in *MICCAI 2014*.
- [25] P. Krähenbühl and V. Koltun. “Efficient inference in fully connected CRFs with Gaussian edge potentials” in *Advances in Neural Information Processing Systems*, pp. 109–117. 2012.
- [26] S. Kumar and M. Hebert. “Discriminative random fields” in *International Journal of Computer Vision*, 68(2):179–201, 2006. ISSN 0920-5691.
- [27] J.Lafferty,A Macculam and F.Preira”Conditional random fields: Probabilistic models for segmenting and labelling sequence data”in *Proceedings of the Eighteenth International Conference on Machine Learning*, pp. 282–289. Morgan Kaufmann Publishers Inc., 2001.
- [28] Y. Boykov and V. Kolmogorov “An experimental comparison of min-cut/maxflow algorithms for energy minimization in vision”in *IEEE Transactions on Pattern Analysis and Machine Intelligence*, 26(9):1124–1137, 2004.
- [29] N. Komodakis,Nikos Paragois and Gergios Tizirtas”MRF energy minimization and beyond via dual decomposition” in *IEEE Transactions on Pattern Analysis and Machine Intelligence*, 33(3):531–552, 2011.
- [30] Philippi Krähenbühl and Vladen Koltun, “Efficient inference in fully connected CRFs with Gaussian edge potentials,” in *Advances in Neural Information Processing Systems*, 2012, pp. 109–117.
- [31] Jose Ignacio Orlando\*, Elena Prokofyeva, and Matthew B. Blaschko” A Discriminatively Trained Fully Connected Conditional Random Field Model for Blood Vessel Segmentation in Fundus Images”in *IEEE Transactions On Biomedical Engineering*, Vol. X, No. X, Month 2015.
- [32] U. T. Nguyen,Alauddin B.,Laurence A.F Park and Kotagiri R”An effective retinal blood vessel segmentation method using multi-scale line detection” in *Pattern Recognition*, 46(3):703–715, 2013.
- [33] J. V. Soares,J.J.G Leandro,R.M.Cesar,H.F.Jelinek and M.J Cree “Retinal vessel segmentation using the 2-D Gabor wavelet and supervised classification” in *IEEE Transactions on Medical Imaging*, 25(9), 2006.
- [34] F. Zana and J.-C. Klein.“Segmentation of vessel-like patterns using mathematical morphology and curvature evaluation” in *IEEE Transactions on Image Processing*, 10(7):1010–1019, 2001.
- [35] J. I. Orlando and M. del Fresno “Reviewing preprocessing and feature extraction techniques for retinal blood vessel segmentation in fundus images” in *Mecánica Computacional*, XXXIII (42):2729–2743, 2014.
- [36] G. Azzopardi, N. Strisciuglio, M. Vento, and N. Petkov”Trainable COSFIRE filters for vessel delineation with application to retinal images” in *Medical Image Analysis*, 19(1):46–57, 2015.
- [37] D. Marín, A. Aquino, M. E. Gegúndez-Arias, and J. M. Bravo”A new supervised method for blood vessel segmentation in retinal images by using graylevel and moment invariants-based features”in *IEEE Transactions on Medical Imaging*, 30(1):146–158, 2011.
- [38] M. M. Fraz et al., “An ensemble classification-based approach applied to retinal blood vessel segmentation,” *Biomedical Engineering, IEEE Transactions on*, vol. 59, no. 9, pp. 2538–2548, 2012
- [39] J. Odstrcilik et al., “Retinal vessel segmentation by improved matched filtering: evaluation on a new high-resolution fundus image database” in *IET Image Processing*, vol. 7, no. 4, pp. 373–383, 2013.
- [40] J. Odstrcilik,J.Jan,J.Gazárek and R.Kolář “Improvement of vessel segmentation by matched filtering in colour retinal images,” in *World Congress on Medical Physics and Biomedical Engineering*, September 7-12, 2009, Munich, Germany. Springer, 2009, pp. 327–330.